

## Molecular Theory of the Miscibility of Hydrocarbon Blends

Chandralekha Singh and Kenneth S. Schweizer\*

Department of Materials Science & Engineering and  
Materials Research Laboratory, University of Illinois,  
1304 West Green Street, Urbana, Illinois 61801

Received July 3, 1995

Revised Manuscript Received September 8, 1995

**Introduction.** Elucidation of the molecular factors which control the miscibility of hydrocarbon alloys has been of great scientific and commercial interest for many years.<sup>1,2</sup> Recently, saturated polyolefin blends have been intensively studied experimentally using modern synthetic methods and characterization tools such as small-angle neutron scattering (SANS).<sup>3–7</sup> A variety of complex physical phenomena have been uncovered including failure of group contribution schemes,<sup>3–7</sup> strong deuteration swap effects,<sup>3,7</sup> failure of mean field random copolymer theory,<sup>3,4,7</sup> unusual temperature dependences of the effective  $\chi$ -parameter,<sup>3–5</sup> and negative  $\chi$ -parameters in special olefin blends.<sup>5</sup> As discussed by the experimentalists,<sup>3–7</sup> none of these effects appear understandable based on the simplest, incompressible Flory–Huggins mean field theory. The latter accounts only for the “bare” chemical interactions within a random mixing, constant volume, lattice model framework. Moreover, counter to most experiments,<sup>3–7</sup> this simple theory suggests polyolefins should be miscible, even at low temperatures, since the *bare* enthalpic  $\chi$ -parameter is extremely small due to the fact that olefin monomers have the same chemical formula. Attempts to rationalize the recent blend data based on compressible “equation-of-state” theories<sup>2</sup> (with empirical parameters) have also not been successful.<sup>3–5</sup>

Recently, different interpretations of the non-mean-field behavior cited above have been advanced, including enthalpy-based empirical solubility parameter schemes<sup>3,4</sup> and a nonlocal excess entropic mechanism.<sup>6</sup> Incompressible field theoretic work<sup>8</sup> has suggested the prime importance of nonlocal excess entropy effects within the context of an *athermal*, quasi-universal description of polyolefins. In contrast, liquid state Polymer Reference Interaction Site Model (PRISM) theory<sup>9–12</sup> and computer simulation<sup>13,14</sup> studies suggest excess entropic effects are small for experimentally relevant models, and *correlated* local enthalpic effects control the excess free energy of mixing.<sup>9,10,12,15</sup>

The goal of the present communication is to explore these issues using recently developed “melt-calibrated” chain models which mimic the behavior of real hydrocarbon chains,<sup>16,17</sup> combined with the technically simplest liquid state theory approach. Two fundamental questions are addressed. (1) What is the influence of conformational and *interchain* energetic asymmetries on blend miscibility? (2) Is there microscopic theoretical support for the validity of a solubility parameter approach? What are the nature and origin of “irregular mixing” behavior which signal the inadequacy of such an approach? Our calculations provide a simple framework to understand many of the puzzling experimental trends as a consequence of competing, *nonadditive* asymmetry effects. New strategies for the rational control of compatibility and design of miscible hydrocarbon alloys are also suggested.

**Theoretical Approach and Model.** Our approach to predicting blend miscibility is to employ PRISM

theory for athermal (repulsive hard core) packing correlations combined with a thermodynamic perturbation approximation for the attractive interaction contributions to the free energy of mixing. Based on the free energy route to the thermodynamics,<sup>10,12,18</sup> and under the assumption that the chains remain ideal in the mixture (i.e., adopt a composition-independent intramolecular structure), the effective  $\chi$ -parameter follows from differentiation of the blend free energy per site as<sup>10</sup>

$$\chi = -\frac{1}{2\phi} \frac{\partial^2}{\partial \phi^2} \left\{ \beta F_a + \frac{\beta}{2\rho} \sum_{M,M'} \rho_M \rho_{M'} \int d\vec{r} v_{MM'}(r) g_{MM'}(r) \right\} \equiv \chi_a + \chi_B \quad (1)$$

where  $\phi$  is the volume fraction of A sites,  $\rho$  is the total site number density in the blend,  $\rho_A = \phi\rho$ ,  $\rho_B = (1 - \phi)\rho$ ,  $v_{MM'}(r)$  [ $g_{MM'}(r)$ ] are the attractive tail potentials [interchain radial distribution functions] between species M and M', and  $F_a$  is the excess noncombinatorial blend free energy associated with the repulsive interactions (explicit statistical mechanical expressions are available<sup>10–13</sup>). The second equality defines *athermal* and *thermal*  $\chi$ -parameters. The spinodal instability corresponds to the condition  $\chi N = 2$  for a  $\phi = 1/2$  and  $N_A = N_B = N$  binary mixture. Thermodynamic perturbation theory, or the so-called high-temperature approximation (HTA), has been adopted in eq 1 corresponding to the physical assumption that the intermolecular packing is determined entirely by the steric repulsive forces.<sup>18</sup> This approximation is particularly appropriate for high molecular weight polymer blends.<sup>19,20</sup> In specific applications to experimental systems, the athermal  $g(r)$ 's depend implicitly on  $T$  via the reduced density and chain aspect ratios. Prior PRISM and computer simulation studies of SFC model mixtures have found that the excess entropic  $\chi_a$  is small and not important for experimentally relevant chain lengths and conformational asymmetries.<sup>9–13</sup> Hence, we drop it and focus solely on the correlated enthalpy contribution  $\chi_B$ . Thus, PRISM theory with the Percus–Yevick closure<sup>18,21</sup> is employed only to compute the pair correlation functions associated with *local* hard core packing, a problem for which it provides very accurate predictions when compared with exact computer simulations of athermal melts<sup>16,22</sup> and blends.<sup>13,14</sup>

In the specific numerical applications, we employ the “melt-calibrated” discrete semiflexible chain (SFC) model<sup>16</sup> discussed in depth elsewhere.<sup>17</sup> We believe this is a minimalist model in the sense it captures the essential conformational (local and global) and intermolecular attractive energy differences between real polymer molecules within a computationally and conceptually simple intermediate-level description.<sup>17</sup> The homopolymer SFC model is characterized by a site hard core diameter  $d$ , a nearest neighbor bond length  $L = d/2$ , bond bending energy  $E_b$ , and degree of polymerization  $N$ . These parameters are chosen so that based on PRISM theory the resultant model accurately mimics *both* the single-chain conformational characteristics *and* the average carbon center *interchain* packing in the melt.<sup>17</sup> The key conformational parameter is the chain aspect ratio defined as  $\Gamma = \sigma/d$ , where  $\sigma^2 = 6R_g^2/N$  and  $R_g$  is the radius of gyration. For flexible hydrocarbon polymers a rather narrow range of  $\Gamma = 0.8$ – $1.4$  is relevant.<sup>10,17</sup> For simplicity, we consider a 50/50 binary blend composed of A and B species of identical degrees of polymerization. The A and B chains are character-

ized by different aspect ratios,  $\Gamma_A$  and  $\Gamma_B$ , which mimic the conformational asymmetries associated with differences in backbone characteristic ratio and monomer structure (e.g., shape, branching). More precise connections with specific polymers have been discussed elsewhere,<sup>10,17</sup> but are not the primary focus of this brief communication. For example,  $\Gamma \approx 1.2$  for polyethylene (PE) and 1.0 for poly(ethylene) (PEE). A "structural asymmetry" variable is defined as  $\Delta\Gamma = \Gamma_B - \Gamma_A$  or  $\gamma = \Gamma_B/\Gamma_A$ ; a mean aspect ratio is  $\Gamma_{av} = (\Gamma_A + \Gamma_B)/2$ .

Each elementary site of a chain interacts *intermolecularly* via a pair-decomposable hard core repulsion plus attractive tail potential. The hard core diameters of the A and B monomers are taken to be equal, and the tail potentials are given by the shifted Lennard-Jones-like form:  $v_{MM'}(r) = \epsilon_{MM'}[x^{-12} - 2x^{-6}]$ , where  $x = r/d$  and  $\epsilon_{MM'} > 0$  quantifies the attractive van der Waals interaction for sites of type M and M' when in contact. The energetic or chemical asymmetry between the species is characterized by the ratio parameter  $\lambda^2 = \epsilon_{BB}/\epsilon_{AA}$ , which can be estimated based on group contribution<sup>23</sup> or molar attraction constant<sup>24</sup> tables and the known monomer structure. For example,  $\lambda \approx 1.04$  for a PE/PEE blend. In principle, the cross energy  $\epsilon_{AB}$  is also an independent, system-specific variable. However, in the spirit of considering a minimalist model, we adopt the Berthelot estimate  $\epsilon_{AB} = (\epsilon_{BB}\epsilon_{AA})^{1/2} = \lambda\epsilon_{AA}$ .

The reduced liquid density is chosen to be  $\rho d^3 = 1.375$ , which guarantees an experimentally realistic *melt* compressibility.<sup>17</sup> For simplicity, we assume the excess volume of mixing is zero and the reduced blend density is composition-independent. Thus, for fixed  $N$ , bulk density, and blend composition, our minimalist model is characterized by two chain structural parameters,  $\Delta\Gamma$  and  $\Gamma_{av}$  (or equivalently  $\Gamma_A$  and  $\Gamma_B$ ), and one energetic asymmetry parameter  $\lambda$ . Temperature enters in a dimensionless form as  $k_B T/\epsilon_{AA}$ . Our present goal is to determine the effective  $\chi$ -parameter, and hence the spinodal boundary, as a function of the three parameters  $\Delta\Gamma$ ,  $\Gamma_{av}$ , and  $\lambda$ .

Before discussing the numerical results, it is instructive to express the thermal  $\chi$ -parameter in terms of two distinct contributions

$$\chi_B = -\frac{\beta\rho}{2} \int d\vec{r} v_{AA}(r) \{g_{AA}(r) + \lambda^2 g_{BB}(r) - 2\lambda g_{AB}(r)\} + \Delta\chi_B \quad (2)$$

where the second term is implicitly defined. Incompressible Flory theory is recovered if a literal mean field approximation is invoked, i.e.,  $g_{MM}(r) = 1$ , resulting in a "bare"  $\chi_0 = (10\pi/9)\rho d^3\beta\epsilon_{AA}(\lambda - 1)^2$ , where  $\beta^{-1}$  is the thermal energy. The first term in eq 2 includes non-random packing corrections and arises from taking compositional derivatives *only* on the factor  $\rho_M\rho_{M'}$  in eq 1. The second term in eq 2 describes enthalpic contributions associated with composition-dependent *changes* in *local* blend (athermal) packing.

Within the above thermodynamic perturbative framework, to obtain a solubility parameter theory requires *two additional* approximations.<sup>25</sup> The "diagonal"  $M = M'$  contributions to  $\chi_B$  in eq 1 are computed using the *pure one-component* melt radial distribution functions, and the AB cross term is approximated by the geometric combining law involving the pure component diagonal terms. [This latter approximation does not have the same theoretical basis as its microscopic energy analog  $\epsilon_{AB} = (\epsilon_{BB}\epsilon_{AA})^{1/2}$ .] Under the above conditions, the

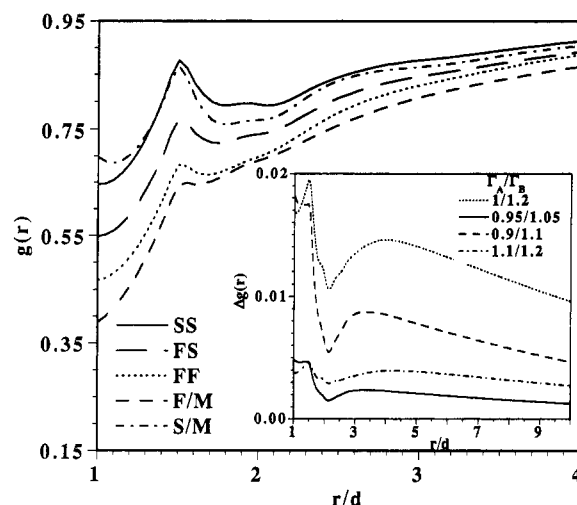


**Figure 1.** Intermolecular site-site pair correlation functions for  $\Gamma = 1.0$  (F) and 1.2 (S) chains in a 50/50 blend and their respective melts (M). The inset shows the intermolecular pairing function defined in the text for four choices of aspect ratios.

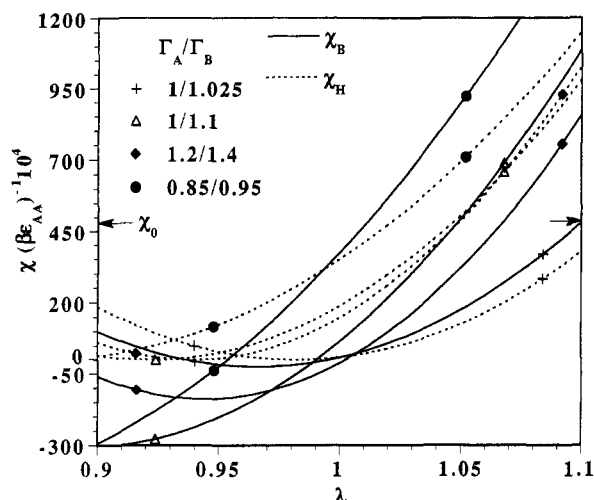
second term in eq 2 vanishes, and the first term reduces to a "Hildebrand  $\chi$ -parameter"

$$\chi_H \equiv \frac{\beta}{2}(\delta_B - \delta_A)^2; \quad \delta_M^2 \equiv -\rho \int d\vec{r} v_{MM}(r) g_{M,m}(r) \quad (3)$$

where  $g_{M,m}(r)$  denotes the athermal *pure melt* radial distribution function of species M and melt cohesive energy parameters have been defined. Note that differences between our computed  $\chi_B$  and  $\chi_H$  arise *solely* from the consequences of the two additional approximations mentioned above. Although  $\chi_H$  can never be negative, subtle competitions between the conformational and energetic asymmetries can occur since *local* chain architecture enters via its influence on the radial distribution functions. This point has been analytically discussed within an idealized Gaussian thread model framework, and qualitative consistency with much of the non-mean-field experimental observations has been demonstrated.<sup>10,17</sup> However, this prior work does *not* address why a microscopic Hildebrand-like theory should work, or its range of validity and the nature of the deviations from a multicomponent statistical mechanical calculation.

**Results and Discussion.** We have carried out extensive model calculations of blend pair correlations and effective  $\chi$ -parameters. Here we present the most important results for  $N = 2000$  and  $\phi = 0.5$ . A full discussion, including many applications to specific experiments, will be given elsewhere.<sup>26</sup>

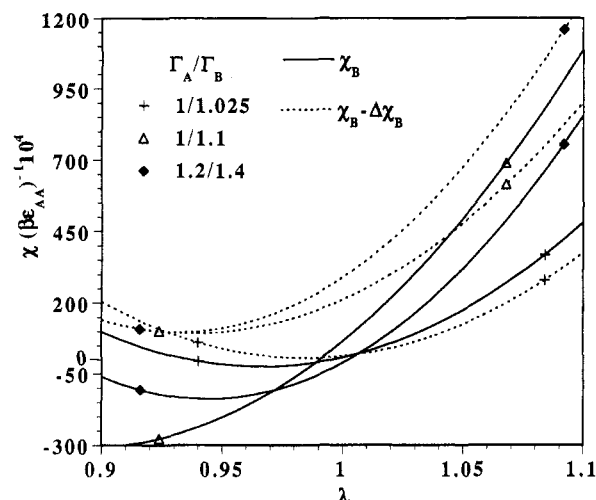
Figure 1 presents results for interchain site-site pair correlations. There are at least three important features. (1) Locally,  $g(r)$  is larger for the higher aspect ratio species, as expected based on standard entropic packing arguments.<sup>16,18,21</sup> (2) Significant changes of the melt AA and BB pair correlations can occur upon blending. In the example shown, the packing of the more flexible chain is enhanced locally, while the stiffer chain is much more weakly perturbed. We caution that the precise magnitude and direction of the local structural changes are nonuniversal.<sup>11,12</sup> (3) The tendency for clustering of like species can be quantified by the function  $\Delta g(r) = g_{AA}(r) + g_{BB}(r) - 2g_{AB}(r)$ , which is



**Figure 2.** Calculated blend (solid line) and Hildebrand (dashed line)  $\chi$ -parameters in units of the reduced thermal energy as a function of the chemical asymmetry variable for four cases of structural asymmetry. The symbols attached to the curves are guides to the eye for identifying the various cases. The arrow labeled  $\chi_0$  shows the mean field Flory prediction (see text) for  $\lambda = 0.9$  and  $1.1$ .

shown in the inset. This function is remarkably small in absolute magnitude, but even values of  $10^{-3}$  produce values of  $\chi_B$  which are significant for high polymers since the melt cohesive energy is of order  $k_B T$ . The tendency for local clustering increases strongly as the stiffness mismatch  $\Delta\Gamma$  increases, but is a weak function of mean aspect ratio at fixed  $\Delta\Gamma$ . These athermal structural correlations are the key input into our theory of the enthalpic  $\chi$ -parameter and blend miscibility.

In Figure 2 we present representative results for the dependence of the blend and Hildebrand  $\chi$ -parameters on chain aspect ratios and the energetic asymmetry variable  $\lambda$ . Simple Flory theory (as discussed in the Introduction) would be a parabola centered about  $\lambda = 1$  and  $\chi = 0$ . The major trends for  $\chi_B$ , and qualitative connection to experiments, are as follows. (1) The  $\chi$ -parameter is predicted to be a nonadditive, nonmonotonic function of the conformational and energetic asymmetry variables. (2)  $\chi_B$  is relatively large and positive when the structural and energetic asymmetries "reinforce", i.e.,  $\gamma > 1$  and  $\lambda > 1$ . This situation corresponds to the physical statement that the larger aspect ratio, "better packing" polymer is also characterized by more attractive van der Waals interaction. In polyolefins, chain branching tends to reduce the effective aspect ratio and weaken the interchain attractions,<sup>10,12,17,23</sup> so a large fraction of possible hydrocarbon alloys are in the "reinforcement regime". These features, plus trend (1) above, immediately lead to the prediction of a "deuteration swap" effect,<sup>3,4</sup> i.e.,  $\chi_B$  increases when the more flexible chain is deuterated (increase of  $\lambda$ ) and  $\chi_B$  decreases when the stiffer chain is deuterated (decrease of  $\lambda$ ). (3) A minimum  $\chi$ -parameter occurs for an optimal value of chemical asymmetry which is in the vicinity of the minimum of  $\chi_H$  (corresponding to equality of melt solubility parameters). (4) Negative values of  $\chi_B$  are predicted when the structural and chemical asymmetries are sufficiently large and if the system is in a "compensation regime", defined as  $\gamma > 1$  and  $\lambda < 1$ , or vice versa. This unexpected result suggests novel strategies for achieving miscibility of hydrocarbon polymers of significantly different monomer structures, and may provide a theoretical basis for understanding certain polyisobutylene blends<sup>5</sup> which



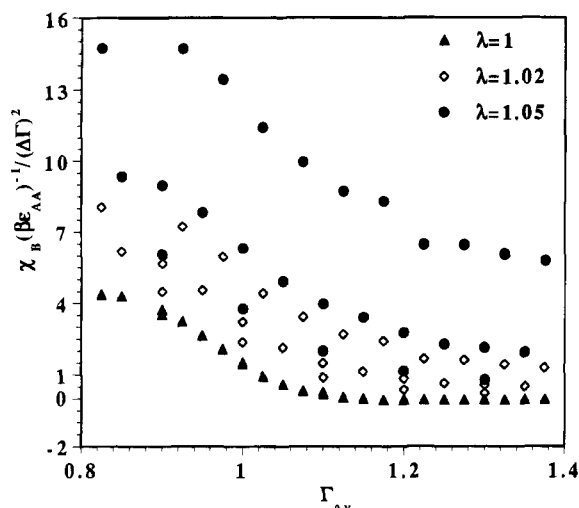
**Figure 3.** Same format as Figure 2, but a comparison of the full blend prediction with the first term in eq 2.

exhibit low  $T$  values of  $\chi$  as small as  $-0.01$ . (5) In the reinforcement regime, the positive  $\chi$ -parameter increases strongly as  $\Delta\Gamma$  increases and decreases as mean aspect ratio increases at fixed structural asymmetry. The latter trend provides a basis for understanding the origin of the failure of random copolymer theory for binary blends of PE/PEE random copolymers and related systems.<sup>3,4,7</sup> (6) Since the factor  $\beta\epsilon$  is of order 1 at typical temperatures,<sup>10,17</sup> our predicted absolute magnitudes are consistent with experiments.<sup>3,4,6</sup> (7) A non-mean-field  $T$ -dependence of  $\chi_B$  may occur due to polymer-specific thermal variations of aspect ratios.

The second major issue addressed in Figure 2 is the relation between the full blend prediction for the enthalpic  $\chi$ -parameter and the microscopic Hildebrand solubility parameter calculation. In the asymmetry reinforcement region characteristic of most olefin blends there is good agreement, which provides theoretical support for the validity of the two additional approximations required to obtain a solubility parameter theory discussed above eq 3. The level of agreement between  $\chi_B$  and  $\chi_H$  tends to improve as the structural mismatch decreases and/or the mean aspect ratio increases. However, significant differences occur as the compensation regime is approached and/or entered. The "negative" deviations ( $\chi_B < \chi_H$ ) are generally predicted to be larger, which perhaps provides a theoretical basis for the observed mixing irregularities.<sup>3,4</sup>

The origin of the rich predictions for  $\chi_B$  is the two terms in eq 3. In Figure 3 the differing behaviors of these two contributions are displayed by comparing the first term in eq 2 with  $\chi_B$ . The first term is an enthalpic contribution of a simple mean field exchange energy form, but with nonunity pair correlation functions. In the asymmetry reinforcement region, this contribution is the largest and is qualitatively similar to  $\chi_H$ . However, near or in the compensation regime the second term,  $\Delta\chi_B$ , can change sign and become dominant. Thus, the physical origin of a  $\chi_B < 0$  is the composition-dependent changes in blend packing.

An attempt to find simple relations, or a data collapse, of our numerical results outside the strong asymmetry compensation regime is presented in Figure 4.  $\chi_B$  divided by a measure of the conformational asymmetry is plotted versus the mean aspect ratio for several choices of the chemical asymmetry variable relevant to polyolefins and three experimentally relevant values of  $\Delta\Gamma$ . The characteristic shape is qualitatively the same



**Figure 4.** Scaled blend  $\chi$ -parameter versus average blend aspect ratio for three values of the chemical asymmetry variable. Results are shown for three values of  $\Delta\Gamma = 0.05$ , 0.1, and 0.2. At fixed  $\Gamma_{av}$ , the value of  $\chi_B/[(\beta\epsilon_{AA})(\Delta\Gamma)^2]$  decreases monotonically with  $\Delta\Gamma$ .

for all cases, and implies that at fixed aspect ratio difference  $\chi_B$  increases as  $\Gamma_{av}$  decreases. This trend is the origin of the failure of random copolymer theory, and is in good accord<sup>10,26</sup> with polyolefin experiments.<sup>3,4</sup> Very good superposition is found for the  $\lambda = 1$  "chemical symmetric" case. At fixed  $\lambda$  the quality of the collapse of different  $\Delta\Gamma$  blends decreases with increasing chemical asymmetry, but collapse of the  $\lambda$  dependence at fixed  $\Delta\Gamma$  improves as the structural asymmetry increases. Even in the worse case, well over an order of magnitude variation in  $\chi_B$  is reduced to a factor of 2–3 variation in  $\chi_B/(\Delta\Gamma)^2$ .

The influence of several physical features on the results of our minimalist model/theory remain to be carefully determined. These include (i) atomistic polymer structural features<sup>12,13,17</sup> such as explicit chain branching, (ii) mixing volume changes, (iii) nonideal conformational perturbations in the blend, and (iv) possible  $T$ -dependent modifications of local packing (beyond HTA).<sup>9,20</sup> Detailed, quantitative applications to many polyolefin blends are in progress and will be reported in the future.<sup>26</sup> Preliminary results show encouraging agreement between the rich experimental behavior and our minimalist theory. However, there are cases not well treated which primarily involve *particular* homopolymer/homopolymer blends with small positive  $\chi$ -parameters, possibly reflecting highly specific local blend packing effects which are not adequately captured by a coarse-grained SFC model. Finally, we suspect our theory will also be useful for understanding the miscibility of polydiene alloys<sup>27</sup> and the local architecture dependence of the microphase separation transition temperature of block copolymers.<sup>6</sup>

**Acknowledgment.** Funding was provided by the Division of Materials Sciences, Office of Basic Energy Sciences, U.S. Department of Energy. Use of the central computer facilities of the Illinois Materials Research Lab (DEFG02-91ER45439) is gratefully acknowledged.

## References and Notes

- (1) Olabisi, O.; Robeson, L. M.; Shaw, M. *Polymer-Polymer Miscibility*; Academic Press: New York, 1979. Koningsveld, R. *Adv. Colloid Interface Sci.* **1968**, *2*, 151.
- (2) Sanchez, I. C.; Lacombe, R. H. *J. Phys. Chem.* **1976**, *80*, 2352, 2368. Walsh, D. J.; Rostami, S. *Adv. Polym. Sci.* **1985**, *70*, 119.
- (3) Graessley, W. W.; Krishnamoorti, R.; Balsara, N. P.; Fetters, L. J.; Lohse, D. J.; Schulz, D.; Sissano, J. *Macromolecules* **1994**, *27*, 2574, 3073, 3896, and references cited therein.
- (4) Graessley, W. W.; Krishnamoorti, R.; Reichart, G. C.; Balsara, N. P.; Fetters, L. J.; Lohse, D. J. *Macromolecules* **1995**, *28*, 1260.
- (5) Krishnamoorti, R.; Graessley, W. W.; Fetters, L. J.; Garner, R. J.; Lohse, D. J. *Macromolecules* **1995**, *28*, 1252.
- (6) Bates, F. S.; Schulz, M. F.; Rosedale, J. *Macromolecules* **1992**, *25*, 5547. Gehlsen, M. D.; Bates, F. S. *Ibid.* **1994**, *27*, 3611.
- (7) Rhee, J.; Crist, B. *Macromolecules* **1991**, *24*, 5663. Nicholson, J. C.; Fineman, T. M.; Crist, B. *Polymer* **1990**, *31*, 2287.
- (8) Bates, F. S.; Fredrickson, G. H. *Macromolecules* **1994**, *27*, 1065. Fredrickson, G. H.; Liu, A. J.; Bates, F. S. *Ibid.* **1994**, *27*, 2503. Fredrickson, G. H.; Liu, A. J. *J. Polym. Sci., Polym. Phys.* **1995**, *33*, 1203.
- (9) Schweizer, K. S. *Macromolecules* **1993**, *26*, 6050.
- (10) Schweizer, K. S.; Singh, C. *Macromolecules* **1995**, *28*, 2063.
- (11) Singh, C.; Schweizer, K. S. *J. Chem. Phys.* **1995**, *103*, 5814.
- (12) Rajasekharan, J. J.; Curro, J. G.; Honeycutt, J. D. *Macromolecules* **1995**, *28*, 6843.
- (13) Weinhold, J.; Kumar, S. K.; Singh, C.; Schweizer, K. S. *J. Chem. Phys.*, in press.
- (14) Stevenson, C. S.; Curro, J. G.; McCoy, J. D.; Plimpton, S. J. *J. Chem. Phys.* **1995**, *103*, 1200, 1208.
- (15) Kacker, N.; Weinhold, J.; Kumar, S. K. *J. Chem. Soc., Faraday Trans.* **1995**, *91*, 2457.
- (16) Honnell, K. G.; Curro, J. G.; Schweizer, K. S. *Macromolecules* **1990**, *23*, 3496.
- (17) Schweizer, K. S.; David, E. F.; Singh, C.; Curro, J. G.; Rajasekharan, J. J. *Macromolecules* **1995**, *28*, 1528.
- (18) Chandler, D. *Studies in Statistical Mechanics VIII*; Montroll, E., Lebowitz, J., Eds.; North-Holland: Amsterdam, The Netherlands, 1982; p 274 and references cited therein.
- (19) Chandler, D. *Phys. Rev. E* **1993**, *48*, 2893.
- (20) Singh, C.; Schweizer, K. S.; Yethiraj, A. *J. Chem. Phys.* **1995**, *102*, 2187.
- (21) Schweizer, K. S.; Curro, J. G. *Phys. Rev. Lett.* **1988**, *60*, 809. Schweizer, K. S.; Curro, J. G. *Adv. Polym. Sci.* **1994**, *116*, 319.
- (22) Curro, J. G.; Schweizer, K. S.; Grest, G.; Kremer, K. *J. Chem. Phys.* **1989**, *91*, 1357. Yethiraj, A.; Hall, C. K. *Ibid.* **1991**, *93*, 4453; **1992**, *96*, 797.
- (23) Coleman, M. M.; Serman, C. J.; Bhagwagar, D. E.; Painter, P. C. *Polymer* **1990**, *31*, 1187.
- (24) Ben-Amotz, D.; Willis, K. G. *J. Phys. Chem.* **1993**, *93*, 7736.
- (25) Hildebrand, J.; Scott, R. *The Solubility of Nonelectrolytes*, 3rd ed.; Reinhold: New York, 1949. For a discussion in the context of modern liquid state theory, see ref 10.
- (26) Singh, C.; Schweizer, K. S., in preparation.
- (27) See, for example: Sakurai, S.; Jinnai, H.; Hasegawa, H.; Hashimoto, T.; Han, C. C. *Macromolecules* **1991**, *24*, 4839. Tomlin, D. W.; Roland, C. M. *Ibid.* **1992**, *25*, 2994.

MA950941+